environmental microbiology

Environmental Microbiology (2021) **23**(2), 1199–1209 doi:10.1111/1462-2920.15348

Special Issue Article

Microscale heterogeneity of the soil nitrogen cycling microbial functional structure and potential metabolism

Shun Han,[1] Xuesong Luo,[2] Xiuli Hao,[1,2] Yang Ouyang,[3] Luyang Zeng,[2] Li Wang,[2] Shilin Wen,[4] Boren Wang,[4] Joy D. Van Nostrand,[3] Wenli Chen ,[1*] Jizhong Zhou[3] and Qiaoyun Huang [1,2*]

[1]*State Key Laboratory of Agricultural Microbiology, Huazhong Agricultural University, Wuhan, China.*

[2]*Key Laboratory of Arable Land Conservation (Middle and Lower Reaches of Yangtze River), Ministry of Agriculture, College of Resources and Environment, Huazhong Agricultural University, Wuhan, China.*

[3]*Department of Microbiology and Plant Biology, School of Civil Engineering and Environmental Sciences, Institute for Environmental Genomics, University of Oklahoma, Norman, OK, 73019.*

[4]*Hengyang Red Soil Experimental Station, Chinese Academy of Agricultural Sciences, Hengyang, 421001, China.*

Summary

Soil aggregates, with complex spatial and nutritional heterogeneity, are clearly important for regulating microbial community ecology and biogeochemistry in soils. However, how the taxonomic composition and functional attributes of N-cycling-microbes within different soil particle-size fractions under a long-term fertilization treatment remains largely unknown. Here, we examined the composition and metabolic potential for urease activity, nitrification, N_2O production and reduction of the microbial communities attached to different sized soil particles (2000–250, 250–53 and <53 μm) using a functional gene microarray (GeoChip) and functional assays. We found that urease activity and nitrification were higher in <53 μm fractions, whereas N_2O production and reduction rates were greater in 2000–250 and 250–53 μm across different fertilizer regimes. The abundance of key N-cycling genes involved in anammox, ammonification, assimilatory and dissimilatory N reduction, denitrification, nitrification and N_2-fixation detected by GeoChip increased as soil aggregate size decreased; and the particular key genes abundance (e.g., *ureC*, *amoA*, *narG*, *nirS/K*) and their corresponding activity were uncoupled. Aggregate fraction exerted significant impacts on N-cycling microbial taxonomic composition, which was significantly shaped by soil nutrition. Taken together, these findings indicate the important roles of soil aggregates in differentiating N-cycling metabolic potential and taxonomic composition, and provide empirical evidence that nitrogen metabolism potential and community are uncoupled due to aggregate heterogeneity.

Introduction

Nitrogen (N) cycling is one of the most crucial biogeochemical cycles and most steps are mediated by microorganisms. Bioavailable N is a critical nutrient in agroecosystems and affects plant growth and crop production. Microbial transformation of N is often depicted as a cycle within soils that requires interaction among microorganisms that carry out N_2-fixation, nitrification (including ammonia oxidation and nitrite oxidation), ammonification, anammox, denitrification, dissimilatory nitrite reduction to ammonia, dissimilatory and assimilatory nitrate reduction (Kuypers *et al*., 2018). Although the diversity and community composition of N-cycling microbes have been studied extensively in terrestrial ecosystems, most have focused on a single step of the N transformation process (e.g., Zehr *et al*., 2003; Zhang *et al*., 2012; Nie *et al*., 2015; Shan *et al*., 2016; Han *et al*., 2017), particularly nitrification and denitrification (He *et al*., 2007a; Shen *et al*., 2008; Kong *et al*., 2010; Jones and Hallin, 2010; Jiang *et al*., 2014; Han *et al*., 2020). However, the coordinative interaction among the abundance, metabolic potential and taxonomic composition of overall N-cycling functional guilds remains elusive in agricultural soils.

Received 31 May, 2020; revised 1 December, 2020; accepted 2 December, 2020. *For correspondence. E-mail wlchen@mail.hzau.edu.cn; qyhuang@mail.hzau.edu.cn; Tel. (+86) 278 728 0670; Fax (+86) 278 728 0670.

Soil exhibits a complex hierarchical structure of pore distribution, oxygen diffusion and aggregate fractions (Zhang *et al*., 2014; Rillig *et al*., 2017). Different sized soil aggregates have spatially heterogeneous habitats with diverse nutrient availability, water retention, oxygen concentration and predation pressure (Sexstone *et al*., 1985; Ranjard and Richaume, 2001; Zhang *et al*., 2014; Jiang *et al*., 2017), which may indirectly induce the shift in abundance, metabolic potential and taxonomic composition of N-cycling microbes. Understanding the extent to which functional guild controls the metabolic process is very important to establishing effective methods to predict microbial activity hotspots at a microscale (e.g., soil aggregate).

Long-term fertilization can affect the spatial heterogeneity of aggregates (Zhang *et al*., 2014), which may influence the succession of soil microbial groups linked to a given biogeochemical process. Previous studies documented that organic fertilization increased the abundance of N-cycling microbes in different sizes soil aggregates: nitrate-reducers and ammonia-oxidizers abundance most abundant in the 63–200 μm size fraction, whereas denitrifiers, ammonifiers and N_2-fixation abundance were highest in the 0.1–2, 2–63 and 200–2000 μm sized fractions respectively (Luo *et al*., 2018). Zhang *et al*. (2017) documented that fertilization treatment and soil aggregate size had a great impact on the abundance of ammonia oxidizers, which significantly increased under organic manure plus chemical fertilizer across all soil fractions. In addition, Kong *et al*. (2010) found that the 63–250 μm sized fractions are microenvironments that promote the growth of nitrifiers and denitrifiers under different N management regimes. While soil aggregate size had no significant effects on nitrite-oxidizer abundance and biodiversity in a red soil (Han *et al*., 2018b), abundance of this group was higher in the 2000–250 and 250–53 μm soil aggregate sizes in a lime concretion black soil (Han *et al*., 2018a). As mentioned above, most research on soil aggregates has focused on subcommunities within the N-cycling functional guilds; however, some rare studies have considered the N-cycling community in its entirety when evaluating the diversity and taxonomic composition and metabolic potential of those systems. In addition, previous studies have focused on a single functional process, such as nitrification or denitrification, ignoring interaction that may be occurring among diverse functional groups and may result in an inaccurate estimation of ecosystem function. Therefore, it is important to investigate overall N-cycling functional guilds to realize a full-scale understanding of the microbial-mediated nitrogen cycle. Large-scale patterns of N-cycling microbial communities suggest that 43%–85% of the spatial variation in the community composition could be better explained by measured environmental factors (mostly soil pH) (Bru *et al*., 2011). However, how the taxonomic composition and functional attributes of N-cycling microbes within different soil particle-size fractions were regulated by the local microhabitat factors under different fertilization regimes remains unclear.

Because of its ability to detect thousands of functional genes simultaneously, numerous studies have utilized the GeoChip to reveal the composition, abundance and dynamics of microbial communities in different ecosystems (Rhee *et al*., 2004; Zhou *et al*., 2012; Xu *et al*., 2014). GeoChip 5.0 (Shi *et al*., 2019), currently the most advanced version of GeoChip, contains 11 398 probes targeting key N-cycling genes. In the present study, we applied the GeoChip 5.0 to decipher the effects of soil aggregate fraction size on N-cycling microbes in a typical Red soil after 26 years of fertilization. We hypothesize that (i) the N-cycling-related functional taxonomic structure and metabolic potential will have shifted based on soil fraction size because of the spatial heterogeneity of the aggregates, (ii) individual N-cycling processes will present different responses to the various soil factors, e.g. soil nitrogen, carbon, potassium and phosphorus.

Results

Potential nitrogen metabolism in soil aggregate under fertilizer regimes

Urease activity was generally higher in the <53 μm size fractions, followed by the 250–53 and then the 2000–250 μm size fractions across the fertilizer regime (Fig. 1A). Compared with the no fertilizer plot (CK), organic fertilizer (M and MNPK) significantly increased urease activity, while inorganic fertilizer (NPK) reduced activity($p < 0.05$), and urease activity could be ranked in the order MNPK>M>CK>NPK. The potential ammonia oxidation activity had a similar trend as the urease activity (Fig. 1B). The potential N_2O production and reduction rates were preferentially higher in the 2000–250 and 250–53 μm fractions, and lowest in the <53 μm size fractions in all plots (Fig. 1C and D). Fertilizer, especially the M treatments, also increased potential N_2O production and reduction rates to varying degrees. Two-way ANOVA showed that those potential nitrogen metabolisms were impacted by both soil aggregate sizes and fertilizer treatment (Table S1). Correlation analysis demonstrated that soil carbon, nitrogen, potassium and phosphorus contents had strong linkages with potential nitrogen metabolisms (Fig. S1).

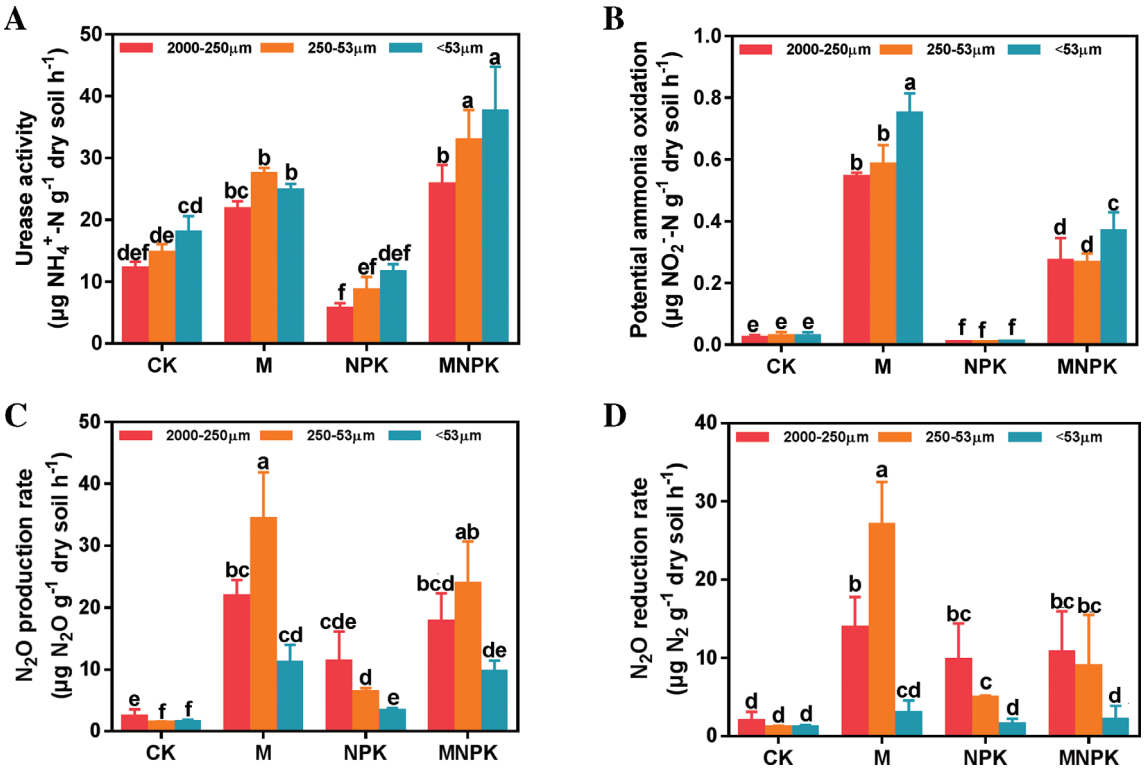

Fig. 1. The key process of N transformation in soil aggregates under diverse fertilizer treatments. Soil urease activity (A), ammonia oxidation activity (B), N_2O production rate (C) and N_2O production rate (D). Error bars represent standard error and are accompanied by lowercase letters indicating significant differences according to Tukey's test ($p < 0.05$). [Color figure can be viewed at wileyonlinelibrary.com]

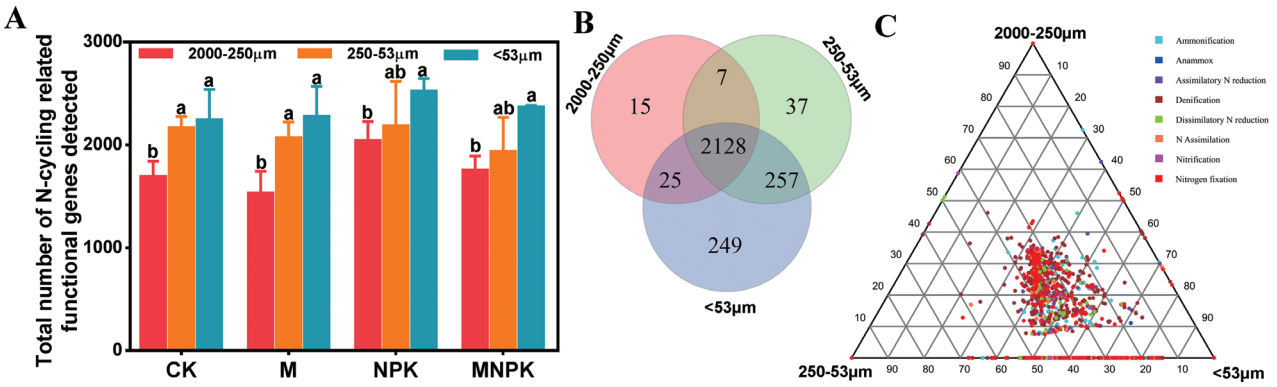

Fig. 2. Total normalized signal intensities of detected genes involved in the N-cycle (A). Error bars represent standard error and are accompanied by lowercase letters indicating significant differences according to Tukey's test ($p < 0.05$). Venn diagram showing the distribution of detected probes among the three different soil aggregates sizes (B). Ternary plot showing the distribution of detected probes involved in N-cycle with a different functional process under soil aggregate levels (C). [Color figure can be viewed at wileyonlinelibrary.com]

N-cycling genes within soil aggregates under different fertilization regimes

The GeoChip detected a total of 2718 N-cycling genes in this experiment, with the largest number detected in the <53 μm size fraction, followed by the 250–53 and 2000–250 μm size fractions in all fertilization regimes (Fig. 2A). This same pattern was observed for individual N transformation processes, for example, ammonification, assimilatory N reduction and denitrification (Table 1). Two-way ANOVA data indicated that the normalized signal intensities were mostly influenced by the soil aggregate size, then by fertilizer treatment (Table S2). Specifically, based on the detected N-cycling genes, e.g. *ureC*, *amoA* and *nosZ*, aggregate size

showed a profound effect ($p < 0.05$) on the abundance of the soil N-cycling microbes across the fertilization treatment (Fig. 3, Fig. S2). These results indicated that soil aggregate size was the most important factor shaping the abundance pattern of the N-cycling genes. In addition, we found that the abundance of *ureC*, *amoA*, *narG*(*nirS*/*K*) and *nosZ* genes did not have a significant relationship with urease activity, potential nitrification, N_2O production and reduction rate respectively (data not shown).

To further analyse the distribution of N-related genes among the three soil aggregate size fractions, a Venn diagram was employed to show the variation (Fig. 2B). Briefly, 78.29% of the N-related genes (2128) were detected in all samples. The <53 μm fraction had a much larger number of unique genes (249; 9.2%) compared with the 2000–250 (15; 0.5%) and 250–53 μm fractions (37; 1.3%). Ternary plots displayed the distribution of detected genes in the three aggregate fractions (Fig. 2C). Those probes detected in the <53 μm fraction were mostly related to N_2 fixation (61 genes, 14.87% of all detected N_2 fixation genes), denitrification (112, 7.93%) and dissimilatory N reduction (13, 9.15%).

Differences of N-cycling-related microbial taxonomic structure in soil aggregates

The Shannon diversity indices of the N-cycling microbial community showed no significant differences among soil

Table 1. Distribution of key gene categories involved in nitrogen cycling.

Gene category	Number of genes											
	2000–250 μm				250–53 μm				250–53 μm			
	CK	M	NPK	MNPK	CK	M	NPK	MNPK	CK	M	NPK	MNPK
Ammonification	278bc ± 5	245c ± 22	320a ± 14	287ab ± 12	340a ± 10	324ab ± 13	329ab ± 19	300b ± 13	347b ± 18	347b ± 8	388a ± 2	369ab ± 2
Anammox	6ab ± 0	5bc ± 0	7a ± 1	3c ± 0	9a ± 0	6bc ± 1	7ab ± 1	5c ± 0	10a ± 1	8b ± 1	9a ± 0	9a ± 1
Assimilatory N reduction	126bc ± 2	116b ± 12	159a ± 10	136ab ± 6	166a ± 6	161a ± 5	161a ± 14	142a ± 7	169b ± 15	171b ± 2	191a ± 0	186ab ± 1
Denitrification	832b ± 30	771b ± 84	981a ± 58	889ab ± 39	1092a ± 39	1036ab ± 39	1025ab ± 78	935b ± 35	1102a ± 87	1119a ± 39	1207a ± 3	1209a ± 3
Dissimilatory N reduction	67b ± 1	61b ± 8	88a ± 9	77ab ± 3	99a ± 3	96a ± 5	92ab ± 7	81b ± 3	99a ± 10	104a ± 4	113a ± 2	112a ± 1
Nitrification	23b ± 1	18b ± 3	27ab ± 2	30a ± 1	30a ± 1	26ab ± 1	29a ± 3	22a ± 1	32a ± 2	29a ± 2	30a ± 1	30a ± 1
Nitrogen fixation	213b ± 5	176c ± 22	261a ± 21	213b ± 14	283a ± 9	263ab ± 15	277a ± 25	233b ± 9	296b ± 23	286b ± 10	347a ± 1	315ab ± 2

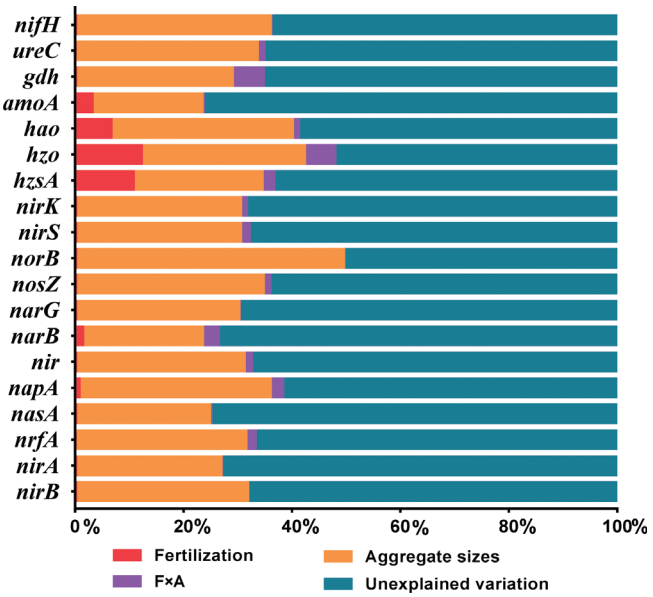

Fig. 3. The comparison of individual and interactive effects of fertilization and soil aggregate sizes on the abundance of N-cycling-related genes. The letters F and A denote fertilization and aggregate sizes respectively. [Color figure can be viewed at wileyonlinelibrary.com]

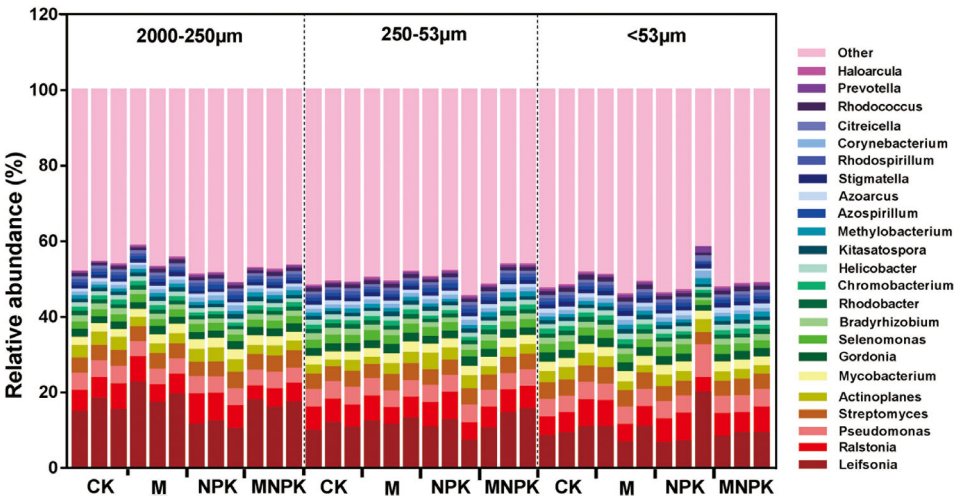

Fig. 4. Taxonomic composition of the N-cycling-related microbial community detected by GeoChip at the genus level. [Color figure can be viewed at wileyonlinelibrary.com]

aggregate samples, suggesting the alpha diversity was relatively stable across microhabitat variation (Fig. S3). The general taxonomic composition of the N-cycling microbes was shown at the genus levels (relative abundance) based on the GeoChip data. In total, 421 genera were detected from all samples (Fig. 4). The dominant genes derived from *Chromobacterium*, *Helicobacter*, *Prevotella*, *Rhodococcus*, *Corynebacterium*, *Methylobacterium*, *Selenomonas* and *Pseudomonas* genus and were higher in the <53 μm fractions. The relative abundance *Leifsonia* and *Actinoplanes* genus were higher in the 2000–250 μm fractions.

Principal component analysis (PCA) explained 45.2% of the total variation in the N-cycling communities (Fig. 5A). The separation of N-cycling community groups along PC1 could be dominantly explained by the aggregate size class variation. In addition, the community from the NPK treatment was differentiated from those of the CK, MNPK and M treatments along the PC2. Furthermore, the N-cycling microbial taxonomic composition was also shaped by soil aggregate sizes at single fertilizer plot (Fig. S4). Consistently, the composition of the N-related microbial community differed remarkably ($p < 0.005$) among soil aggregate fraction size, as indicated by multiple non-parametric dissimilarity tests [analysis of similarities (ANOSIM), ADONIS and multires ponse permutation procedure (MRPP)] based on Bray–Curtis dissimilarity (Table 2). Permutational multivariate analysis of variance (PERMANOVA) results also indicated that the N-related microbial community composition was considerably ($p < 0.05$) shifted by both long-term fertilization and aggregate size, but that aggregate size exhibited more pronounced effects ($p < 0.01$) (Fig. 5B). All these results suggest that the soil N-cycling community was dramatically altered in the different aggregate size classes and by fertilization.

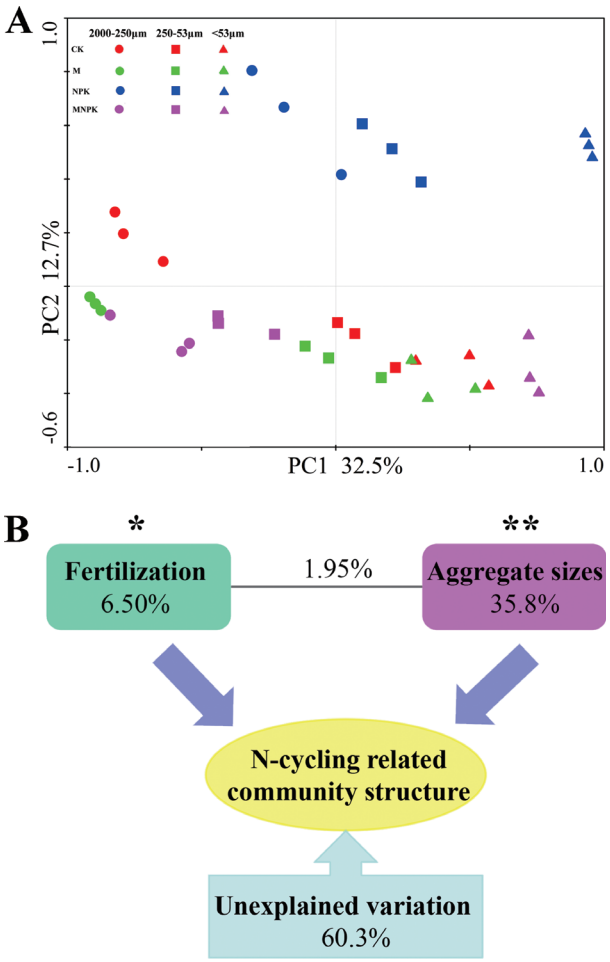

Fig. 5. Principal component analysis (PCA) of the detected N-cycle-related functional genes at all soil samples (A). Permutational multivariate analysis of variance (PERMANOVA) comparing the main and interactive effects of fertilization and soil aggregate sizes on the community composition of N-cycling-related microbial (999 permutations) (B). Stars denote for significances at $p < 0.05$ and $p < 0.01$ probability levels (* and **, respectively). [Color figure can be viewed at wileyonlinelibrary.com]

Association between the soil variables and microbial functional structure

Significant positive relationships were found between the composition of the N-cycling communities and soil variables in all soil aggregate fractions: total samples ($r = 0.45$, $p < 0.01$), 2000–250 μm ($r = 0.42$, $p < 0.01$), 250–53 μm ($r = 0.56$, $p < 0.01$) and <53 μm ($r = 0.43$, $p < 0.01$) (Fig. S5). To decipher how the soil variables shaped the beta-diversity of the overall N-cycling community, a redundancy analysis (RDA) was performed. Eight soil variables, including soil total carbon (TC), total nitrogen (TN), soil organic carbon (SOC), TP, TK, available phosphorus (AP), available potassium (AK) and NH_4^+-N, were described in our former study (Han *et al*., 2018b). About a third (35.0%) of the constrained variation in the N-related microbial taxonomic composition was explained by the first two axes (Fig. 6A). The N-cycling microbial composition in the three aggregate fractions was mainly separated along the first axis. All soil properties had significant correlations with the microbial functional structures ($p < 0.05$) (Fig. 6B), suggesting nutrient level played a key role in shaping the N-cycling community in a microhabitat. To further explain the correlation between soil variables and the specific subcommunities involved in N-related processes, the Mantel test was performed (Fig. S6). The subcommunities related to nitrification, N_2 fixation, ammonification, dissimilatory N reduction, assimilatory N reduction, denitrification and anammox correlated significantly with soil AP ($p < 0.05$), SOC ($p < 0.05$), TC ($p < 0.05$) and TN ($p < 0.05$), while the anammox subcommunity was correlated significantly with soil AK ($p < 0.01$), TP ($p < 0.01$) and C:N ratio ($p < 0.01$). Moreover, the nitrification subcommunity was significantly correlated to soil C:N ($p < 0.05$) and TP ($p < 0.05$). No significant relationships were found among the subgroups and NH_4^+-N or TK content.

Table 2. Non-parametric analyses to test dissimilarity of communities based on Bray–Curtis dissimilarity among soil aggregate fractions.

	ANOSIM		ADONIS		MRPP	
	R	*p*	*F*	*p*	*δ*	*p*
2000–250 μm vs 250–53 μm	0.32	0.001	19.7	0.001	0.12	0.002
2000–250 μm vs <53 μm	0.42	0.001	19.3	0.001	0.14	0.001
250–53 μm vs <53 μm	0.46	0.001	23.5	0.001	0.11	0.002

Discussion

Soil aggregates could provide spatially heterogeneous habitats for many microorganisms, including those that are involved in N-cycling-related functions. These particle-associated populations may have important impacts on the utilization and loss of nitrogen as well as greenhouse gas emissions under different climate change regimes. Since this is an area that has not been well studied, we examined how the microenvironmental heterogeneity of soil aggregates affected the functional and taxonomic biodiversity of N-cycling microbial communities and their metabolic potential under long-term fertilization of an agro-ecosystem.

Potential nitrogen metabolism hotspots depend on soil aggregate size

In this study, we found that the <53 μm size fractions were hotspots for urease activity and nitrification, while the 2000–250 and 250–53 μm fractions were hotspots for potential N_2O production and reduction regardless of the fertilizer regime. This finding contradicts that of Wang *et al*. (2018), which showed urease activity was highest

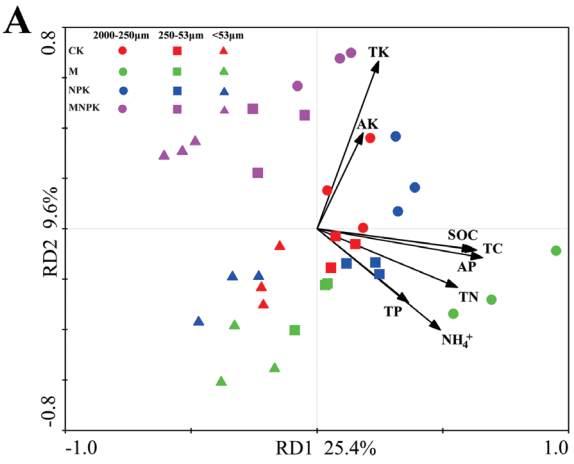

B

Monte Carlo permutation test

	F	*P*
TC	5.44	<0.01
TN	4.45	<0.01
SOC	5.09	<0.01
TP	3.02	<0.01
AP	4.94	<0.01
TK	2.47	<0.05
AK	2.46	<0.05
NH_4^+	3.31	<0.01

Fig. 6. Redundancy analyses of detected N-cycle-related functional genes at all soil samples with selected environmental variables (A). Eight soil variables were selected: TC, TN, SOC, TP, TK, AP, AK and NH_4^+-N. Monte Carlo permutation test with 999 unrestricted permutations was used to test the significance of statistics (B). [Color figure can be viewed at wileyonlinelibrary.com]

in the 250–53 μm fractions and lowest in the <53 μm fraction of a Black soil. However, similar to our results, Jiang *et al*. (2014) documented an increase in potential nitrification as the soil aggregate size decreased. Nitrification is an aerobic process, so this phenomenon may be at least partly explained by the greater surface-to-volume ratio of smaller soil aggregates, which may increase O_2 availability. In contrast, larger soil aggregates may be a more suitable microhabitat for potential N_2O production and reduction due to their smaller surface-to-volume ratio (Schlüter *et al*., 2018) and anaerobic centre (Sexstone *et al*., 1985). Therefore, soil aggregate size may indirectly determine whether an aerobic or anaerobic nitrogen metabolic process occurs by directly regulating oxygen availability, further differentiating microbial hotspots.

Differentiation of microbial functional genes due to soil aggregate sizes

Whether N-cycling processes differ based on soil particle size is a critical issue. In this study, the N-cycling genes had a homogeneous response to soil particle size. All the N-cycling genes had significantly higher intensities in the <53 μm fraction, followed by those in the 250–53 μm fraction and then in the 2000–250 μm fraction under all fertilization regimes. This is in contrast to a previous study that showed that the abundance of N-cycling prokaryotic groups had a heterogeneous response to differently sized soil particles and fertilization treatment (Luo *et al*., 2018). Specifically, the genes involved in ammonification (*gdh*), nitrification (*amoA*), denitrification (*narG*, *nirK*, *nirS* and *norB*) and dissimilatory N reduction (*napA*) had the highest abundance in the 200–63 μm fractions exposed to organic fertilizer compared with that with NPK. Previous studies have also reported that *amoA*, involved in nitrification, had the lowest abundance values in the <250 μm fractions (Jiang *et al*., 2014) and 2–0.1 μm fractions (Zhang *et al*., 2017). Kong *et al*. (2010) also found that the 250–63 μm size fraction had microenvironments that promoted the growth of nitrifiers and denitrifiers under different N management regimes. Due to differences in soil type, land management practices and methodology among the different studies, it is difficult to identify a consistent trend in the accumulated data.

Soil microbes generally live in close vicinity to or attached to soil particles, which may provide a favourable microhabitat for them to access nutrients and growth substrates (Mills, 2003; Young *et al*., 2008). In the present study, the abundance of key N-cycling genes was inversely proportional to the size of the soil particles under different fertilization regimes. A similar trend was observed with the Shannon diversity index as well. This could be because the smaller-sized soil particles are generally bound together by an extracellular polysaccharide matrix that produces independent compartments where microorganisms interact on a small spatial scale (Zhang *et al*., 2015). These separate compartments may provide the bacteria shelter from predators and outside interference (Oades, 1984; Postma and Veen, 1990), resulting in an increase of bacterial biomass in the <53 μm fractions compared with that of the larger fractions (Sessitsch *et al*., 2001). In addition, the smaller aggregates can communicate better with the bulk soil and with other aggregates, due to the smaller surface-to-volume ratio (Schlüter *et al*., 2018), which may also increase diversity. The bacterial taxonomic distribution in soil particles may affect the microbial biodiversity and biological activity at microscales (Neumann *et al*., 2013; Vos *et al*., 2013; Ling *et al*., 2014).

Potential N metabolism activities uncoupled with functional gene abundance of the soil aggregates

Based on our experimental results, N-cycling functional gene abundance was uncoupled from its corresponding potential metabolisms. There are some possible reasons to be mentioned. Soil aggregate size could affect the surface-to-volume ratio (Schlüter *et al*., 2018) and further affect oxygen availability (such as diffusion rate), which can impact the aerobic and anaerobic N metabolism within or/and on the surface of soil aggregates. Although smaller soil aggregate had a higher relative N-cycling microbial abundance in this study and a greater surface-to-volume ratio, it had a lower soil nutrition level. During the potential activity measurement, the metabolism of within and on surface aggregate nitrogen cycling bacteria could be differently affected by the oxygen and soil nutrition availability. Previous studies also indicated that smaller aggregate size fractions typically contain smaller sized pores, therefore the microbial (e.g., denitrifiers) located in the pores within smaller sized aggregates may have been better protected from predators (Hattori, 1988; Jocteur-Monrozier *et al*., 1991). However, the functional process rate should be controlled by the expression of related genes, rather than their DNA abundance (Rocca *et al*., 2015; Wood *et al*., 2015). Indeed, the expression of a gene could be more fluctuating in response to transient environmental changes, e.g. oxygen availability had been shown to regulate the expression of denitrifying genes (Lycus *et al*., 2018) and the expression of *amoA* could be more diverse than being predicted by the DNA-SIP analysis (Pratscher *et al*., 2010). It should be noticed that soil urease is present as both intracellular and extracellular forms, and the proportion of extracellular urease was estimated to account for 26.9% to 62.9% of total urease activity in soils (Klose and Tabatabai, 1999). Thus,

the uncoupled between the extracellular urease activity measured and GeoChip functional *ureC* gene abundance is understandable.

Effects of soil particles and variables on the taxonomic composition of functional groups

Even though bacterial community composition and biomass have been demonstrated to differ among the different size of soil particles (Sessitsch *et al*., 2001; Liao *et al*., 2018), few studies have focused on whether soil aggregate size and fertilization treatment impacts the taxonomic composition and function of the N-cycling microbes. Our GeoChip data indicated that the taxonomic composition of the overall N-cycling microbial community was shaped by both fertilization and soil aggregate size; moreover, aggregate size exhibited more pronounced effects than fertilization. In contrast, previous research has demonstrated that fertilization type is a major factor influencing the community structure of soil ammonia oxidizers community structure (Jiang *et al*., 2014; Zhang *et al*., 2017), nitrite oxidizers (Han *et al*., 2018a; Han *et al*., 2018b), as well as ammonifiers (Wang *et al*., 2018), while particle size is a secondary factor. Additional studies are needed to further decode the roles of aggregate size and fertilization regime on the overall nitrogen cycling microbial community structure and how other factors may affect that response in different soil types. Soil nutrients were significantly impacted by both different fertilizer regimes and soil aggregate size class (Table S1 from Han *et al*., 2018b), while the functional community was predominantly by aggregate size. The fertilization regimes not only impacted soil pH and total nutrient content but also affected nutrient accumulation pathways (nutrient distribution in soil aggregates) and soil aggregation (Han *et al*., 2018b). For instance, the highest level of TC and TN in the soil was observed in the 2000–250 μm fractions, then followed by the 250–53 and <53 μm fractions. The soil NH_4^+, K, P and SOC content was higher in the 2000–250 and 250–53 μm fractions and lowest in the <53 μm fractions. Therefore, the microhabitat variation (e.g., soil nutrient level, oxygen and water availability) could be the dominant factors that shape the functional community in a certain soil aggregate size fraction. This is supported by our RDA analysis, which showed that N-cycling microbial taxonomic composition significantly correlated with all soil variables including TC, SOC, TN, NH_4^+-N, AP, TP, AK and TK. When analysed by PCA and PERMANOVA, the effects from fertilization seemed small. The direct effect from fertilization on the overall nitrogen cycling community could be hindered (or overlapped) by the microhabitat variation. Indeed, microorganisms in the face of nutrient selection pressure will promote changes in their taxonomic composition (Neumann *et al*., 2013; Jiang *et al*., 2014; Liao *et al*., 2018; Han *et al*., 2020) and soil aggregates providing spatially heterogeneous niches for microbes to occupy (Wilpiszeski *et al*., 2019).

Experimental procedures

Experimental design, soil sampling, soil aggregate fractionation collection and determination of soil properties

The long-term field site was located at the Qiyang Red Soil Experimental Station (N 26°45′N, E 111°52′), Hunan Province, China, and has been used for winter wheat and summer maize rotation since it was established in 1990. Four fertilization treatments were utilized: (i) no fertilizer (CK); (ii) swine manure (M); (iii) chemical fertilizer (nitrogen (N), phosphate (P) and potassium (K) fertilizers, NPK); or (iv) combined chemical/manure fertilizer (NPK and swine manure, MNPK). Nitrogen fertilizer was applied as urea or swine manure at 300 kg N ha^{-1}, phosphate (P) as superphosphate at 53 kg P ha^{-1}, and potassium (K) as potassium chloride at 100 kg K ha^{-1}. Detailed information on the experimental design can be found in Han *et al*. (2018b).

In November 2016, six soil cores (diameter: ~5 cm) at a depth of 0–20 cm were collected from 12 fertilization plots (four fertilization treatments ×3 replicates). Soil samples were stored in a bag and delivered to the laboratory within 24 h after soil sampling, and stored at 4°C refrigerator for no longer than 1 week. Next, water-stable aggregates were manually separated into three fractions by sieving approximately 100 g of fresh soil through a series of sieves (2000–250, 250–53 and <53 μm fractions). The soil aggregates were collected, freeze-dried and stored at −80°C until needed for subsequent experiments. Soil TC, TN, SOC, ammonium (NH_4^+-N), AP and AK, TP and TK were measured as described previously by Han *et al*. (2018b).

Determination of potential nitrogen metabolism in soil aggregates

Soil potential nitrification activity (PNA) was gauged as described by Han *et al*. (2020). Briefly, ~3.0 g soil was incubated in 30 ml of 10 mM $NaClO_3$ (to inhibit nitrite-oxidation) with 2 mM $(NH_4)_2SO_4$ (ammonium sulfate) with gentle shaking (180 rpm) at 28°C. Nitrite accumulation rates during incubation were regarded as the PNA. Soil urease activity data were obtained from Wang *et al*. (2020), which using urea solution as the substrate to assess the urease activity. Soil nitrous oxide (N_2O) production and reduction rates were determined using an acetylene inhibition method as described in Smith and

Tiedje (1979) and Liu *et al*. (2016). Briefly, soil aggregate (~5 g) was incubated with 5 ml solutions, which was contained with glucose [0.5 (mg C) · (g dry soil)$^{-1}$], sodium glutamate [0.5 (mg C) · (g dry soil)$^{-1}$], and KNO_3 [200 (μg NO_3^--N) · (g dry soil)$^{-1}$], put into a 125 ml glass bottle with shaking (180 rpm) at 28°C. Each soil sample was divided into two subsamples with or without C_2H_2 (10% vol./vol.) and was activated by flushing with 99.9% N_2 for 5 min. N_2O concentrations were detected by gas chromatography (Agilent 7890A, Agilent Technologies, Santa Clara, CA, USA). The potential N_2O production rate was calculated within the microcosm supplemented with C_2H_2. The potential N_2O reduction rate was estimated by the difference between the potential N_2O production rate and N_2O production within the microcosm without C_2H_2.

DNA preparation

Microbial community DNA was extracted from 0.5 g soil using a PowerSoil® DNA Isolation Kit following the manufacturer's protocol. Three replicates of DNA extracts were pooled as a single sample. The concentration and quality of DNA were determined using a Quant-It PicoGreen (Invitrogen, Carlsbad, CA) and Nanodrop One spectrophotometer (NanoDrop Technologies, Wilmington, USA) respectively. DNA samples were stored at −80°C for future analysis.

GeoChip 5.0 hybridization and scanning

GeoChip 5.0 (Shi *et al*., 2019), synthesized by Agilent was used to analyse the functional composition and abundance of the microbial communities. Briefly, DNA was labelled with the fluorescent dye Cy3 using a random priming method and purified with a QIA quick purification kit (Qiagen, Valencia, CA, USA) following the manufacturer's instructions. After measuring dye incorporation on a NanoDrop ND-1000 spectrophotometer (Nano-Drop Technologies) DNA was dried in a SpeedVac (ThermoSavant, Milford, MA, USA) at 45°C for 45 min. Then, the labelled DNA was suspended in hybridization buffer, hybridized at 68°C and 10% formamide for approximately 16 h, and then scanned by a NimbleGen MS200 scanner (Roche, Madison, WI, USA) using a laser power and photomultiplier tube gain of 100%. Signal intensities were subsequently quantified using Agilent's Feature Extraction software. Spots with signal-to-noise ratio <2.0 were removed before data analysis, as described formerly (He *et al*., 2010). According to the probes involved in the nitrogen-cycling processes, the probe could be dividing into seven key gene categories, including anammox, ammonification, assimilatory N reduction, denitrification, dissimilatory N reduction, nitrification and nitrogen fixation. The detailed information about those categories was described in He *et al*. (2007a).

Statistical analysis

The impacts of fertilization treatment and soil aggregate size on the number of N-related genes detected and Shannon-diversity index and metabolic potential were analysed using two-way ANOVA with SPSS 19.0 (IBM, Armonk, NY, USA). Venn diagram and ternary plots were drawn to show the distribution of specific probes detected by GeoChip in each soil aggregate. PERMANOVA was employed to reveal the effects of fertilization treatment and soil aggregate size on the community composition and abundance of the N-cycling microbial community by using the 'adonis' function. The differences in microbial functional structure among soil aggregate sizes were performed by PCA, and three non-parametric tests, MRPP, ANOSIM and permutational multivariate analysis of variance (ADONIS) based on Bray–Curtis dissimilarity. The relationship between the microbial functional composition and soil variables was assessed by RDA. The Monte Carlo permutation test with 999 unrestricted permutations was used to test the statistical significance. Mantel test was used to explore the relationship between soil variables and N-cycling processed based on Bray–Curtis dissimilarity. Euclidean distance and Bray–Curtis coefficients were used to construct soil variables and dissimilarity matrices of taxonomic communities respectively. All data analyses were performed with R v.3.2.4 (www.R-project.org).

Acknowledgements

This work was supported by the National Key Research and Development Program of China (2018YFE0105600), the National Natural Science Foundation of China (42020104003). The authors wish to thank the Qiyang Red Soil Experimental Station staff for sampling assistance and managing the field experiments, as well as the anonymous reviewers for constructive comments.

Author Contributions

QYH, WLC and SH designed the project and collected soil samples. QYH and WLC provided supervision and funding acquisition. SH performed the experiment with the help of LYZ and LW. SH performed the data analyses. BRW and SLW managed the experiment field. QYH, WLC, JDVN and JZZ completed writing-review and editing. SH wrote the manuscript in consultation with QYH, WLC, XSL, XLH, YOY, JDVN and JZZ.

References

Bru, D., Ramette, A., Saby, N.P.A., Dequiedt, S., Ranjard, L., Jolivet, C., *et al*. (2011) Determinants of the distribution of nitrogen-cycling microbial communities at the landscape scale. *ISME J* **5**: 532–542.

Han, S., Li, X., Luo, X., Wen, S., Chen, W., and Huang, Q. (2018b) Nitrite-oxidizing bacteria community composition and diversity are influenced by fertilizer regimes, but are independent of the soil aggregate in acidic subtropical red soil. *Front Microbiol* **9**: 885.

Han, S., Luo, X., Liao, H., Nie, H., Huang, Q., and Chen, W. (2017) *Nitrospira* are more sensitive than *Nitrobacter* to land management in acid, fertilized soils of a rapeseed-rice rotation field trial. *Sci Total Environ* **599**: 135–144.

Han, S., Luo, X., Tan, S., Wang, J., Chen, W., and Huang, Q. (2020) Soil aggregates impact nitrifying microorganisms in a vertisol under diverse fertilization regimes. *Eur J Soil Sci* **71**: 536–547.

Han, S., Xiong, X., Luo, X., Zeng, L., Wei, D., Chen, W., and Huang, Q. (2018a) Fertilization rather than aggregate size fractions shape the nitrite-oxidizing microbial community in a Mollisol. *Soil Biol Biochem* **124**: 179–183.

Hattori, T. (1988) Soil aggregates as microhabitats of microorganisms. *Rep Inst Agric Res Tohoku Univ* **37**: 23–36.

He, J., Shen, J., Zhang, L., Zhu, Y., Zheng, Y., Xu, M., *et al*. (2007a) Quantitative analyses of the abundance and composition of ammonia-oxidizing bacteria and archaea of a Chinese upland red soil under long term fertilization practices. *Environ Microbiol* **9**: 2364–2374.

He, Z., Gentry, T., Schadt, C., Wu, L., Liebich, J., Chong, S., *et al*. (2007b) GeoChip: a comprehensive microarray for investigating biogeochemical, ecological and environmental processes. *ISME J* **1**: 67–77.

He, Z., Xu, M., Deng, Y., Kang, S.H., Kellogg, L., Wu, L., *et al*. (2010) Metagenomic analysis reveals a marked divergence in the structure of belowground microbial communities at elevated CO_2. *Ecol Lett* **13**: 564–575.

Jiang, Y., Jin, C., and Sun, B. (2014) Soil aggregate stratification of nematodes and ammonia oxidizers affects nitrification in an acid soil. *Environ Microbiol* **16**: 3083–3094.

Jiang, Y., Liu, M., Zhang, J., Chen, Y., Chen, X., Chen, L., *et al*. (2017) Nematode grazing promotes bacterial community dynamics in soil at the aggregate level. *ISME J* **11**: 2705–2717.

Jocteur-Monrozier, L.J., Ladd, J.N., Fitzpatrick, R.W., Foster, R.C., and Raupach, M. (1991) Components and microbial biomass content of size fractions in soil of contrasting aggregation. *Geoderma* **49**: 37–62.

Jones, C.M., and Hallin, S. (2010) Ecological and evolutionary factors underlying global and local assembly of denitrifier communities. *ISME J* **4**: 633–641.

Klose, S., and Tabatabai, M.A. (1999) Urease activity of microbial biomass in soils. *Soil Biol Biochem* **31**: 205–211.

Kong, A.Y.Y., Hristova, K., Scow, K.M., and Six, J. (2010) Impacts of different N management regimes on nitrifier and denitrifier communities and N cycling in soil microenvironments. *Soil Biol Biochem* **42**: 1523–1533.

Kuypers, M.M., Marchant, H.K., and Kartal, B. (2018) The microbial nitrogen-cycling network. *Nat Rev Microbiol* **16**: 263–276.

Liao, H., Zhang, Y., Zuo, Q., Du, B., Chen, W., Wei, D., *et al*. (2018) Contrasting responses of bacterial and fungal communities to aggregate-size fractions and long-term fertilizations in soils of northeastern China. *Sci Total Environ* **635**: 784–792.

Ling, N., Sun, Y., Ma, J., Guo, J., Zhu, P., and Peng, C. (2014) Response of the bacterial diversity and soil enzyme activity in particle-size fractions of mollisol after different fertilization in a long-term experiment. *Biol Fert Soils* **50**: 901–911.

Liu, Y., Liu, Y., Zhou, H., Li, L., Zheng, J., Zhang, X., *et al*. (2016) Abundance, composition and activity of denitrifier communities in metal polluted paddy soils. *Sci Rep* **6**: 19086.

Luo, G., Friman, V.P., Chen, H., Liu, M., Wang, M., Guo, S., *et al*. (2018) Long-term fertilization regimes drive the abundance and composition of N-cycling-related prokaryotic groups via soil particle-size differentiation. *Soil Biol Biochem* **116**: 213–223.

Lycus, P., Soriano-Laguna, M.J., Kjos, M., Richardson, D.J., Gates, A.J., Milligan, D.A., *et al*. (2018) A bet-hedging strategy for denitrifying bacteria curtails their release of N_2O. *Proc Natl Acad Sci U S A* **115**: 11820–11825.

Mills, A.L. (2003) Keeping in touch: microbial life on soil particle surfaces. *Adv Agron* **78**: 1–43.

Neumann, D., Heuer, A., Hemkemeyer, M., Martens, R., and Tebbe, C.C. (2013) Response of microbial communities to long-term fertilization depends on their microhabitat. *FEMS Microbiol Ecol* **86**: 71–84.

Nie, S., Li, H., Yang, X., Zhang, Z., Weng, B., Huang, F., *et al*. (2015) Nitrogen loss by anaerobic oxidation of ammonium in rice rhizosphere. *ISME J* **9**: 2059–2067.

Oades, J.M. (1984) Soil organic matter and structural stability: mechanisms and implications for management. *Plant Soil* **76**: 319–337.

Postma, J., and Veen, J.A.V. (1990) Habitable pore space and survival of Rhizobium leguminosarum biovar trifolii introduced into soil. *Microb Ecol* **19**: 149–161.

Pratscher, J., Dumont, M.G., and Conrad, R. (2010) Ammonia oxidation coupled to CO_2 fixation by archaea and bacteria in an agricultural soil. *Proc Natl Acad Sci U S A* **108**: 4170–4175.

Ranjard, L., and Richaume, A.S. (2001) Quantitative and qualitative microscale distribution of bacteria in soil. *Res Microbiol* **152**: 707–716.

Rhee, S.-K., Liu, X., Wu, L., Chong, S.C., Wan, X., and Zhou, J. (2004) Detection of genes involved in biodegradation and biotransformation in microbial communities by using 50-mer oligonucleotide microarrays. *Appl Environ Microbiol* **70**: 4303–4317.

Rillig, M.C., Muller, L.A.H., and Lehmann, A. (2017) Soil aggregates as massively concurrent evolutionary incubators. *ISME J* **11**: 1943–1948.

Rocca, J.D., Hall, E.K., Lennon, J.T., Evans, S.E., Waldrop, M.P., Cotner, J.B., *et al*. (2015) Relationships between protein-encoding gene abundance and corresponding process are commonly assumed yet rarely observed. *ISME J* **9**: 1693–1699.

Schlüter, S., Henjes, S., Zawallich, J., Bergaust, L., Horn, M., Ippisch, O., *et al*. (2018) Denitrification in soil aggregate analogues-effect of aggregate size and oxygen diffusion. *Front Environ Sci* **6**: 17.

Sessitsch, A., Weilharter, A., Gerzabek, M.H., Kirchmann, H., and Kandeler, E. (2001) Microbial population structures in soil particle size fractions of a long-term fertilizer field experiment. *Appl Environ Microbiol* **67**: 4215–4224.

Sexstone, A.J., Revsbech, N.P., Parkin, T.B., and Tiedje, J.M. (1985) Direct measurement of oxygen profiles and denitrification rates in soil aggregates. *Soil Sci Am J* **49**: 645–651.

Shan, J., Zhao, X., Sheng, R., Xia, Y., Ti, C., Quan, X., *et al*. (2016) Dissimilatory nitrate reduction processes in typical Chinese paddy soils: rates, relative contributions, and influencing factors. *Environ Sci Technol* **50**: 9972–9980.

Shen, J., Zhang, L., Zhu, Y., Zhang, J., and He, J. (2008) Abundance and composition of ammonia-oxidizing bacteria and ammonia-oxidizing archaea communities of an alkaline sandy loam. *Environ Microbiol* **10**: 1601–1611.

Shi, Z., Yin, H., Van Nostrand, J.D., Voordeckers, J.V., Tu, Q., Deng, Y., *et al*. (2019) Functional gene array-based ultrasensitive and quantitative detection of microbial populations in complex communities. *mSystems* **4**: e00296-19.

Smith, M.S., and Tiedje, J.M. (1979) Phases of denitrification following oxygen depletion in soil. *Soil Biol Biochem* **11**: 261–267.

Vos, M., Wolf, A.B., Jennings, S.J., and Kowalchuk, G.A. (2013) Micro-scale determinants of bacterial diversity in soil. *FEMS Microbiol Rev* **37**: 6–54.

Wang, L., Luo, X., Liao, H., Chen, W., Wei, D., Cai, P., and Huang, Q. (2018) Ureolytic microbial community is modulated by fertilization regimes and particle-size fractions in a black soil of northeastern China. *Soil Biol Biochem* **116**: 171–178.

Wang, L., Xiong, X., Luo, X., Chen, W., Wen, S., Wang, B., *et al*. (2020) Aggregational differentiation of ureolytic microbes in an Ultisol under long-term organic and chemical fertilizations. *Sci Total Environ* **716**: 137103.

Wilpiszeski, R.L., Aufrecht, J.A., Retterer, S.T., Sullivan, M. B., Graham, D.E., Pierce, E.M., *et al*. (2019) Soil aggregate microbial communities: towards understanding microbiome interactions at biologically relevant scales. *Appl Environ Microbiol* **85**: e00324-19.

Wood, S.A., Bradford, M.A., Gilbert, J.A., McGuire, K.L., Palm, C.A., Tully, K.L., *et al*. (2015) Agricultural intensification and the functional capacity of soil microbes on smallholder African farms. *J Appl Ecol* **52**: 744–752.

Xu, M., Zhang, Q., Xia, C., Zhong, Y., Sun, G., Guo, J., *et al*. (2014) Elevated nitrate enriches microbial functional genes for potential bioremediation of complexly contaminated sediments. *ISME J* **8**: 1932–1944.

Young, I.M., Crawford, J.W., Nunan, N., Otten, W., and Spiers, A. (2008) Microbial distribution in soils: physics and scaling. *Adv Agron* **100**: 81–121.

Zehr, J.P., Jenkins, B.D., Short, S.M., and Steward, G.F. (2003) Nitrogenase gene diversity and microbial community structure: a cross-ystem comparison. *Environ Microbiol* **5**: 539–554.

Zhang, H., Ding, W., He, X., Yu, H., Fan, J., and Liu, D. (2014) Influence of 20-year organic and inorganic fertilization on organic carbon accumulation and microbial community structure of aggregates in an intensively cultivated sandy loam soil. *PLoS One* **9**: e92733.

Zhang, L., Hu, H., Shen, J., and He, J. (2012) Ammonia-oxidizing archaea play more important role than ammonia-oxidizing bacteria in ammonia oxidation of strongly acidic soils. *ISME J* **6**: 1032–1045.

Zhang, Q., Liang, G., Myrold, D.D., and Zhou, W. (2017) Variable responses of ammonia oxidizers across soil particle-size fractions affect nitrification in a long-term fertilizer experiment. *Soil Biol Biochem* **105**: 25–36.

Zhang, Q., Zhou, W., Liang, G., Sun, J., Wang, X., and He, P. (2015) Distribution of soil nutrients, extracellular enzyme activities and microbial communities across particle-size fractions in a long-term fertilizer experiment. *Appl Soil Ecol* **94**: 59–71.

Zhou, J., Xue, K., Xie, J., Deng, Y., Wu, L., Cheng, X., *et al*. (2012) Microbial mediation of carbon-cycle feedbacks to climate warming. *Nat Clim Change* **2**: 106–110.

Supporting Information

Additional Supporting Information may be found in the online version of this article at the publisher's web-site:

Appendix S1. Supporting Information.